Development 122, 449-460 (1996)
Printed in Great Britain © The Company of Biologists Limited 1996
DEV3338

Functional cooperation between the non-paralogous genes *Hoxa-10* and *Hoxd-11* in the developing forelimb and axial skeleton

Bertrand Favier, Filippo M. Rijli, Catherine Fromental-Ramain, Valérie Fraulob, Pierre Chambon* and Pascal Dollé

Institut de Génétique et de Biologie Moléculaire et Cellulaire, CNRS/INSERM/ULP, Collège de France, BP 163-67404 Illkirch-Cedex, CU de Strasbourg, France

*Author for correspondence

SUMMARY

The *Abdominal B*-related *Hoxa-10* gene displays similar expression patterns in the differentiating forelimbs and hindlimbs of the mouse, with preferential expression around the humeral and femoral cartilages and more diffuse expression in distal regions. We found that a targeted disruption of *Hoxa-10* has almost no effect in the forelimbs, while it affects the proximal hindlimb skeleton. The alterations were located along the dorsolateral side of the femur (labium laterale), with an enlargement and distal shift of the third trochanter, a misshapen lateral knee sesamoid, a supernumerary 'ligament' connecting these structures and an occasional duplication of the femoral trochlea. Some *Hoxa-10*$^{-/-}$ mutant mice developed severe degenerative alterations of the knee articulation upon ageing. Viable *Hoxa-10/Hoxd-11* double mutant mice were produced by genetic intercrosses. The compound mutation resulted in synergistic forelimb phenotypic alterations, consisting of: (i) an exacerbation of *Hoxd-11*$^{-/-}$ phenotypic traits in the carpal and digital region, e.g. more pronounced truncations of the ulna styloid, pyramidal and pisiform bones and of some metacarpal and phalangeal bones and (ii) marked alterations in a more proximal region which is nearly unaffected in *Hoxd-11*$^{-/-}$ single mutants; the entire radius and ulna were truncated and thickened, with deformations of the ulna proximal extremity. Thus, functional redundancy can occur even between non-paralogous *Abdominal B*-related *Hox* genes. The double *Hoxa-10/Hoxd-11* mutation also conferred full penetrance to the sacral and caudal vertebrae transformations which are ~50% penetrant in *Hoxd-11*$^{-/-}$ single mutants, revealing that functional cooperation can also occur between non-paralogous *Hox* gene products in axial skeleton patterning.

Key words: *Hox* genes, gene disruption, pattern formation, functional redundancy, combinatorial code, *Hoxa-10*, *Hoxd-11*, mouse, axial skeleton, forelimb

INTRODUCTION

Among the 38 members of the murine *Hox* family, 14 genes related to the *Drosophila Abdominal B* gene and located at the 5′ extremity of the *HOXA, HOXC* and *HOXD* complexes are likely to be involved in limb morphogenesis. The *Hoxa* and *Hoxd* genes are activated sequentially, and are expressed in nested proximodistal (P-D) domains along the developing forelimb and hindlimb buds, the most 5′-located gene transcripts being restricted to the autopods (the footplates) of the limbs (Dollé et al., 1989; Haack and Gruss, 1993; Duboule, 1992). The expression patterns of *Hoxc* genes are different from those of their *Hoxa* and *Hoxd* paralogues, and also different in forelimbs and hindlimbs (Peterson et al., 1994). Targeted mutations of *Hoxd-11* (Davis and Capecchi, 1994; Favier et al., 1995), *Hoxd-13* (Dollé et al., 1993) and *Hoxa-11* (Small and Potter, 1993) affect restricted regions of the distal forelimb and hindlimb skeleton, the alterations generated by *Hoxa-11* and *Hoxd-11* mutations extending more proximal than those of the *Hoxd-13* mutation. All three mutations also produced distinct vertebral transformations in the lumbosacral region.

As a '3′-located' *Abdominal B*-related gene, *Hoxa-10* is expressed up to very proximal regions of the developing limbs (Haack and Gruss, 1993; see below). We (Rijli et al., 1995) and others (Satokata et al., 1995) have inactivated the *Hoxa-10* gene and found that this resulted in thoracic and lumbar vertebral transformations, as well as specific genital abnormalities. We describe here the *Hoxa-10* mutant limb phenotype, which is essentially restricted to proximal regions of the hindlimbs. In addition, to investigate whether the expression of *Hoxa-10* up to the distal extremities of the developing limbs is functionally significant, we have produced mice mutated for both *Hoxa-10* and *Hoxd-11* by genetic intercrosses. We show that these two mutations act synergistically to produce marked alterations in the skeletal elements already affected by the *Hoxd-11* mutation, and also in more proximal forelimb regions. Moreover, axial skeletal analysis revealed an increased penetrance in double mutant mice, of the lumbar and sacral transformations

inconsistently found in both single *Hoxa-10* and *Hoxd-11* mutants.

MATERIALS AND METHODS

Hoxa-10 and *Hoxd-11* gene targeting

The production of *Hoxa-10*$^{-/-}$ and *Hoxd-11*$^{-/-}$ mutant mice by homologous recombination in ES cells has been described elsewhere (Rijli et al., 1995; Favier et al., 1995). The *Hoxa-10* gene was disrupted by insertion of a PGK promoter-neomycin resistance minigene into the *Xho*I site of the homeobox. The *Hoxd-11* mutation was generated by inserting a pMC1 neomycin resistance minigene after deletion of the intron and part of the second exon of the gene. Both targeted mutations disrupt the coding sequence within and C-terminal to the homeodomain, thus preventing the synthesis of truncated gene products able to bind DNA.

Double *Hoxa-10/Hoxd-11* mutants were produced by successive intercrosses both in a 129/Sv inbred and a C57BL/6-129/Sv hybrid genetic background. The occurrence of each compound genotype was checked at 3-weeks post-partum. The recorded numbers were compared to those expected from Mendelian inheritance by a χ^2 test.

Skeletal analysis of mutant mice

The alizarin red/alcian blue skeletal staining procedure has been described previously (Dollé et al., 1993). The length of the metacarpals, first and second phalanges of digit II, III, IV and V, radius, ulna, humerus, scapula, metatarsal III, tibia, femur and pelvic belt were recorded for 5 to 7 animals of each compound genotype, either by direct measurements or using a fixed magnification on a display monitor. Bone length reductions were calculated by comparison with the mean length of the left and right corresponding bones of a control animal (wild type (WT) or heterozygous for only one of the two mutations) from the same litter and killed at the same age (3-4 months). Initial comparisons showed no significant bone size alteration in single heterozygous animals compared to WT. The mean reduction rate was then calculated for each genotype. Less extensive data have also been collected for 1-, 3- and 6-day-old double mutant animals.

For the analysis of the vertebral skeleton, the limits of the transformed region was sometimes equivocal because (i) the natural individual variability in mammal vertebral morphology is greater in the lumbar region than at the cervical and the thoracic level (Barone, 1986), (ii) all lumbar vertebrae are very similar to each other, lateral and spinous processes (the more useful features for vertebral rank identification) having a smooth gradient of size and shape from the first lumbar vertebra to the last one, and (iii) these differences between normal lumbar vertebrae of different rank are more subtle than the ones distinguishing, for example, a normal T13 from a transformed T13* (whose ribs have an abnormal caudal curvature). The identification of mutant lumbar vertebrae was based therefore upon the closest morphology of lateral and spinous processes seen in lumbar vertebrae of control skeletons (for iconography, see Fromental-Ramain et al., 1996). We have also used the following morphological landmarks, which showed little variation between control animals: (i) an L3 morphology was assigned to the most anterior vertebra exhibiting lateral processes extending beyond the level of the intervertebral articulation. This criterion was associated with vertebra #23 in 14/17 control skeletons, and twice with vertebra #24, and once with vertebra #22; (ii) an L4 morphology was assigned to the most posterior vertebra harbouring accessory processes. On the L4 vertebra, these processes do not have square extremities like their more anterior counterparts, but have a thin extremity or a small round shape. This criterion was associated with vertebra #24 in 13/17 control skeletons, and once with vertebra #23, twice with vertebra #25 and once unilaterally in vertebrae #24 and #25. The four last thoracic, the sacral and the two first caudal vertebrae were easily recognized, using criteria found in anatomical literature (Barone, 1986; Popesko, 1992). *Hoxa-10*$^{+/-}$ and *Hoxd-11*$^{+/-}$ single heterozygous mutant skeletons were similar to WT ones and thus considered as control in litters lacking WT animals. For each litter, vertebrae of the mutant and control animals were examined for the presence of these landmarks, and their frequency was determined at each level, which allowed us to assign a vertebral phenotype to the various genotypes. As an example of natural variability, note that one of the WT skeletons had only 12 ribs, and 2 out of 17 controls had a T10 with an abnormal morphology. Moreover, whenever asymmetric morphology was recorded for a vertebra, be it from a control or a mutant animal skeleton, the left side had always the more anterior morphology.

RESULTS

Hoxa-10 and *Hoxd-11* transcript expression in the differentiating limbs

The expression pattern of *Hoxa-10* was analyzed in the differentiating limbs (12.5-14.5 days post-coitum, dpc), since previous studies were performed at earlier stages (9.5 to 12.5 dpc; Haack and Gruss, 1993). At these earlier stages, *Hoxa-10* transcripts were preferentially expressed around the differentiating skeletal elements of the proximal segments of the limbs. By 13.5 dpc, strong expression was detected around the cartilaginous blastemas of the femur and the humerus (Fig. 1A). In contrast, *Hoxa-10* transcripts were much more diffuse in distal regions of the limbs and decreased toward the footplates (Fig. 1A). At 14.5 dpc, *Hoxa-10* expression was detected around the femur primordium, with higher transcript levels toward its proximal extremity in the area of the presumptive trochanter (Fig. 1B, open arrows), and around its distal extremity (Fig. 1B). Transcripts of the paralogous gene *Hoxd-10* did not extend more proximally than the presumptive knee area (Fig. 1A,B, arrowheads) and *Hoxa-10* transcripts were more widely distributed than *Hoxd-10* transcripts in the mesenchyme of the developing knee region (Fig. 1B). Similar expression patterns were observed at 14.5 dpc in the developing forelimbs (data not shown; see below).

Hoxa-10 and *Hoxd-11* transcript distribution was also compared on adjacent limb sections. In the forelimbs, *Hoxd-11* transcripts were strongly expressed in the autopod and extended proximally along the posterior half of the zeugopod (Fig. 1C, 12.5 dpc), with a clear expression around the ulna anlage (Fig. 1D, 13.5 dpc). The proximal boundary was at the level of the presumptive elbow, around the distal extremity of the developing humerus (data not shown). *Hoxa-10* was expressed at low levels in the forelimb autopod (Fig. 1C), and at higher levels in the zeugopod, but with a more diffuse distribution than *Hoxd-11* transcripts (Fig. 1C,D) *Hoxa-10* was also expressed around the differentiating humerus (data not shown). Very similar patterns of expression were observed in the hindlimbs, with *Hoxd-11* transcripts extending along the posterior part of the zeugopod including the periphery of the fibula anlage, but not around the tibia anlage (data not shown).

Proximal hindlimb skeletal structures are selectively affected in *Hoxa-10*$^{-/-}$ mutant mice

The proximal part of the femur presents two apophyses which serve as attachment sites for some sublumbar (trochanter minor) and rump (trochanter major) muscles. These two

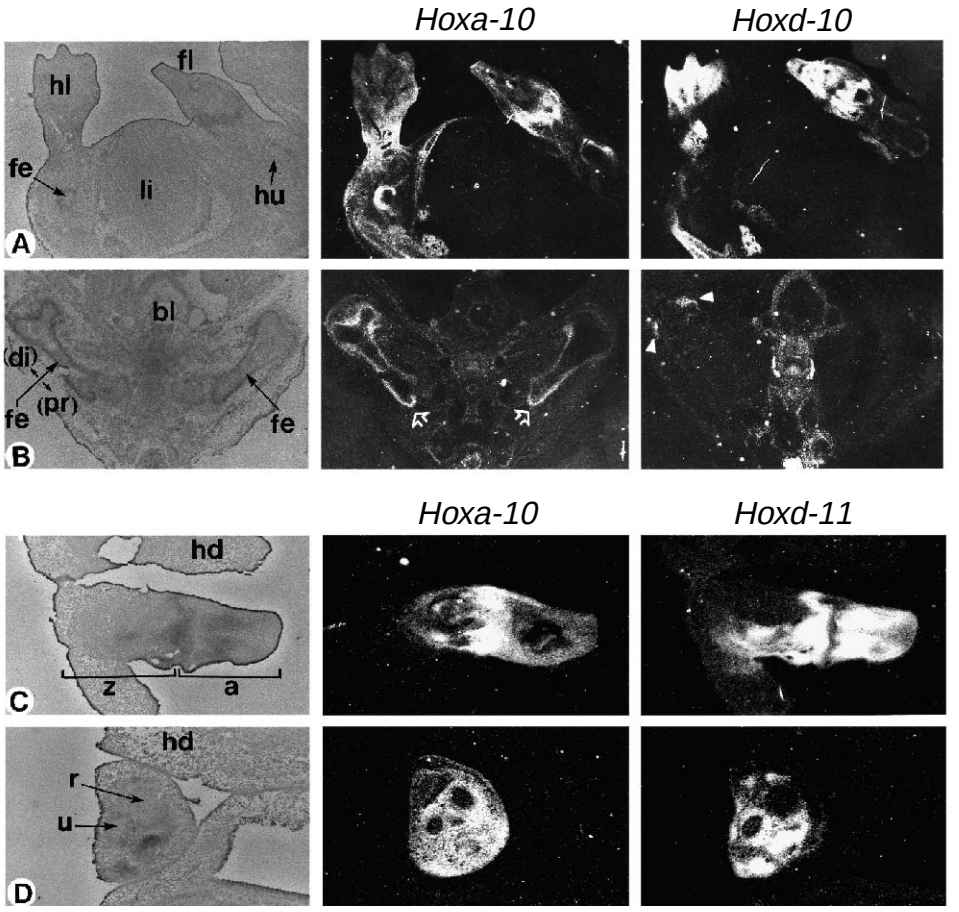

Fig. 1. Comparison of the *Hoxa-10*, *Hoxd-10* and *Hoxd-11* transcript expression domains in differentiating limbs. Left panels are bright-field views showing the histology, and right panels are dark-field views where the silver signal grains appear white. (A) Adjacent sagittal sections through the limbs of a 13.5 dpc fetus, hybridized respectively to a *Hoxa-10* (Haack and Gruss, 1993) and *Hoxd-10* (Duboule and Dollé, 1989) riboprobe. (B) Coronal sections through the hindlimb stylopods of a 14.5 dpc fetus, hybridized to the same probes. The open arrows indicate the preferential expression of *Hoxa-10* in the trochanter area and the arrowheads point to *Hoxd-10* restricted expression in the knee region. (C) Sagittal sections through the forelimb (zeugopod and autopod) of a 12.5 dpc embryo, hybridized respectively to a *Hoxa-10* (Haack and Gruss, 1993) and *Hoxd-11* (Izpisúa-Belmonte et al., 1991) riboprobe. (D) Transverse sections of a 13.5 dpc forelimb at the level of the zeugopod, hybridized to the same probes. a, autopod; bl, urinary bladder; fe, femur [(di), distal; (pr), proximal]; fl, forelimb; hd, head; hl, hindlimb; hu, humerus; li, liver; r, radius; u, ulna; z, zeugopod.

trochanters, as well as the femoral head, appeared normal in *Hoxa-10*$^{-/-}$ mutants (compare Fig. 2A to B,C). However, the third trochanter (trochanter tertius), the insertion site of the m. gluteus superficialis, located along the dorsolateral side (labium laterale) of the femur of *gliridae* (rodents and rabbits) and *equidae*, was altered in 55% of the *Hoxa-10*$^{-/-}$ mutants (Fig. 2B,C). The mutant third trochanter was enlarged, shifted distally and did not present a distinct proximal edge. This alteration was observed in homozygous mutants of both the inbred and hybrid genetic backgrounds (Fig. 2B,C, respectively).

The distal articular surface of the femur consists of two condyles articulating with the tibia, and a trochlea articulating with the patella (Fig. 2D). The femoral condyles were not altered in *Hoxa-10*$^{-/-}$ mutant mice (Figs 2E, 3). The normal trochlea has a unique medial groove (Fig. 2D). In 2 out of 18 mutants with a hybrid genetic background, the trochlea appeared duplicated, with a medial crest separating two symmetrical grooves (Fig. 2E).

Mice have two sesamoid bones at the level of the knee, each facing the femoral condyles at the medial side (ms, Fig. 3A) or lateral side (ls, Fig. 3D). These sesamoids are embedded in the tendons of origin of each gastrocnemius muscle. The medial sesamoid bones of most *Hoxa-10*$^{-/-}$ mutant mice showed variable degrees of size reduction and were unilaterally absent in 3 out of 27 hindlimbs analyzed (Fig. 3B, and data not shown). The lateral sesamoid bones of *Hoxa-10*$^{-/-}$ mutants were misplaced proximally and misshapen, usually displaying a ‘heart shape’ due to an abnormal proximal protrusion (Fig. 3E, curved arrow). Supernumerary ossified structures were also evident in some specimens (Fig. 3F, curved arrow). There was no detectable alteration in the tibia, fibula or hindfeet of *Hoxa-10*$^{-/-}$ mutants.

An abnormal fibrous structure (hereafter called ‘ligament’) was detected along the lateral side of the femur, between the altered third trochanter and the lateral condyle and encompassing the altered lateral sesamoid bone (Fig. 4B, double arrow; visible also in Fig. 3E,F, small arrows). The severity of the lateral sesamoid deformation correlated with the presence of a more pronounced ‘ligament’. We noticed a similar, but thinner and more fragile structure in some control hindlimbs and less affected mutants. Thus, this mutant ‘ligament’ may correspond to an abnormal thickening of the septum intermuscularis femoris lateralis, a duplication of the fascia lata rejoining the femur on its lateral side (Barone, 1986). The muscle gluteus superficialis attaches distally to the third trochanter. In *Hoxa-10*$^{-/-}$ mutants with abnormal third trochanter, its distal tendon was shifted distally and some of its fibers merged into the ectopic ‘ligament’ (data not shown). This may create pathological tension within the ‘ligament’, since the gluteus superficialis muscle is a flexor of the hip, whereas the gastrocnemius, attached at the level of the lateral sesamoid, is an extensor of the tarsal joint, these two movements being antagonistic during locomotion. The resulting impairment in knee mobility may explain why several 8- to 12-month-old *Hoxa-10*$^{-/-}$ mutant mice developed severe degenerative alterations of the knee with numerous signs of

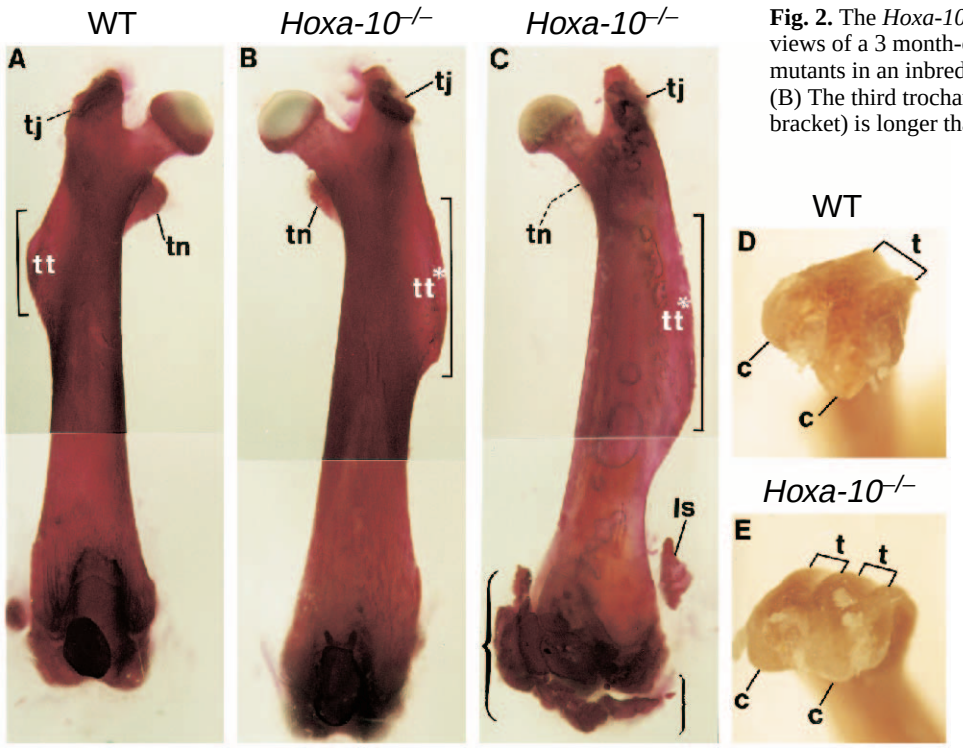

Fig. 2. The *Hoxa-10*$^{-/-}$ femoral phenotype. (A-C) Cranial views of a 3 month-old control (A) and two *Hoxa-10*$^{-/-}$ mutants in an inbred (B) or hybrid (C) genetic background. (B) The third trochanter (trochanter tertius, tt, indicated by a bracket) is longer than in the control, and its shape is mildly altered especially at the proximal edge. (C) The third trochanter is more affected, extending over the middle of the femur shaft and with no clear proximal edge. Braces show abnormal (intracapsular, intraligamentary) ossification of the knee articulation. Because of these, the femur does not have the exact same orientation as in A and B, and the trochanter minor is hidden. (D,E) Distal extremities of a WT (D) and a *Hoxa-10*$^{-/-}$ (E) femur. (D) On the anterior side is the trochlea, where the patella articulates. On the posterior side are the condyles which articulate to the tibia via the menisces. (E) The whole distal extremity of the femur appears enlarged with a duplicated trochlea, but the two condyles seem normal. c, condyle; ls, deformed lateral sesamoid; tj, trochanter major; tn, trochanter minor; tt, trochanter tertius; t, trochlea.

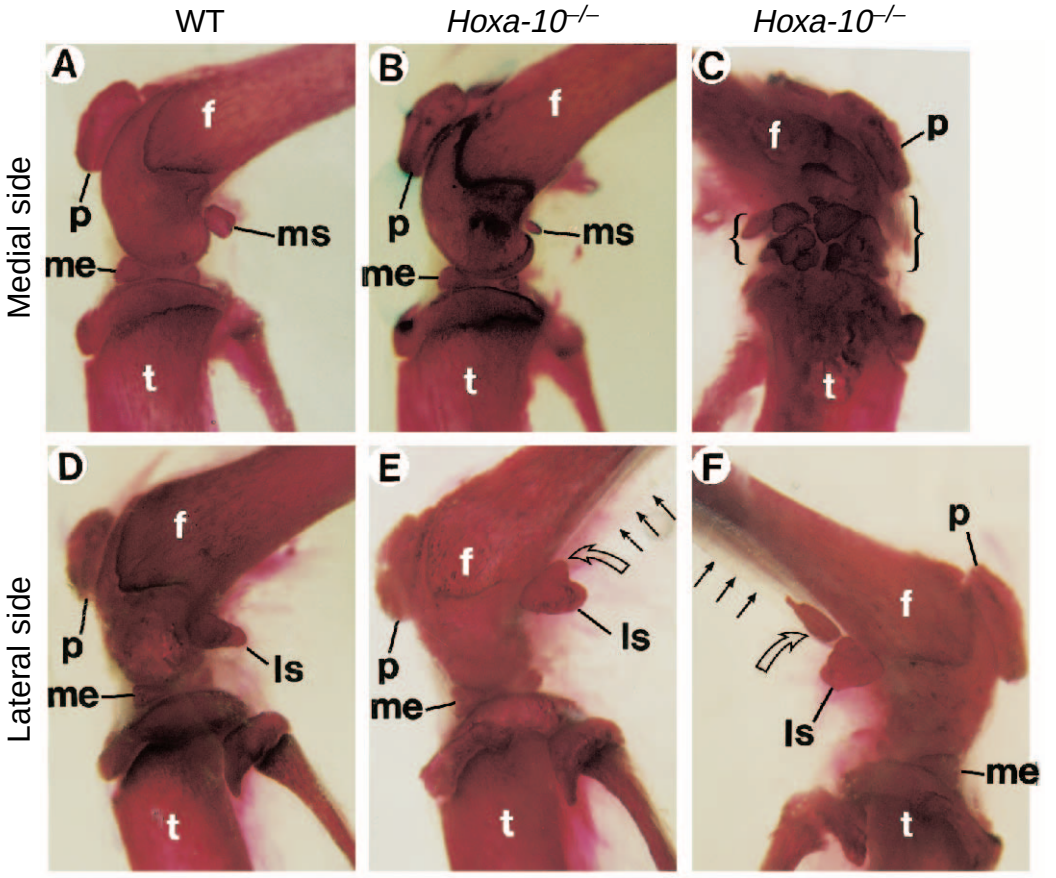

Fig. 3. Knee alterations in *Hoxa-10*$^{-/-}$ mutant mice. (A-C) Medial views of the knee skeleton of a WT (A) and two *Hoxa-10*$^{-/-}$ (B,C) specimens. (B) Reduction of the medial sesamoid, while other structures including the patella and the menisces appear normal. (C) The specimen is older (10 months old) and displays numerous osteophytes and ectopic intracapsular and intraligament ossified structures (indicated by braces). All other animals displayed in this figure are 3-4 months old. (D-F) Lateral views of the knee skeleton of a WT (D) and two *Hoxa-10*$^{-/-}$ (E,F) specimens. The lateral sesamoid is embedded in the tendon of the gastrocnemius muscle lateral caput. (E) The mutant lateral sesamoid has a heart shape and is displaced proximally along the femur shaft. The extra edge (curved arrow) is orientated proximally and is the insertion point of an abnormal 'ligament' still visible after the clearing procedure (three parallel arrows). (F) Notice the altered shape of the lateral sesamoid and the supernumerary sesamoid (curved arrow), embedded in the 'ligament' (three parallel arrows). f, femur; ls, lateral sesamoid; me, meniscus; ms, medial sesamoid; p, patella; t, tibia.

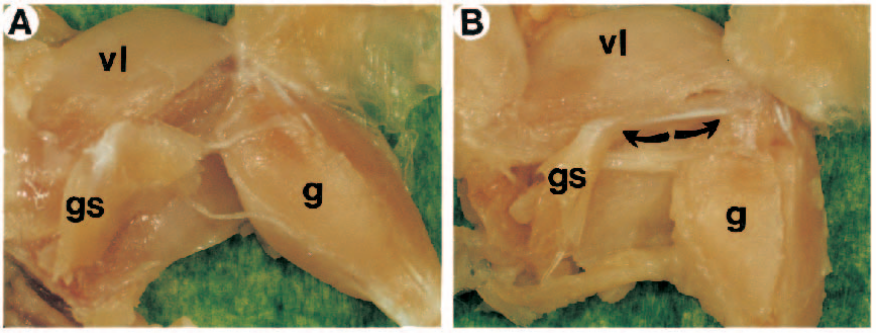

Fig. 4. A supernumerary 'ligament' in *Hoxa-10*$^{-/-}$ hindlimbs. Dissected muscles of the lateral side of a control (A) and a *Hoxa-10*$^{-/-}$ mutant (B) hindlimb. (A) The fascia lata was reclined, the muscle gluteus superficialis (gs) dissected and some caudal muscles removed to expose the gastrocnemius and the caudal side of the vastus lateralis. (B) The same preparation on a *Hoxa-10*$^{-/-}$ mutant revealed a novel 'ligament' (double arrow) extending from the third trochanter, where the gluteus superficialis is attached, to the lateral sesamoid, where the gastrocnemius is attached. g, gastrocnemius muscle; gs, gluteus superficialis muscle; vl, vastus lateralis muscle.

ectopic ossification in the articular capsule, the lateral ligaments and around the patella (Fig. 3C and 2C).

Heterozygous *Hoxa-10*$^{+/-}$ mutants had apparently normal hindlimbs, except for the presence of an altered third trochanter in one limb, and four limbs with a thick but incomplete 'ligament' which did not reach the third trochanter (data not shown).

The only minor abnormality that could be detected in the forelimbs of *Hoxa-10*$^{-/-}$ mutant mice was a somewhat wider humeral deltoid crest in ~25% of the specimens (not shown).

Synergistic effects of the *Hoxa-10 and Hoxd-11* mutations on the generation of forelimb abnormalities

Double mutants were produced by genetic intercrosses. In the F_2 progeny, all compound mutant genotypes were obtained in a Mendelian ratio at the age of three weeks ($\chi^2 = 7.16$, 8 degrees of freedom, out of 161 animals), and no increased lethality was observed thereafter. Thus, *Hoxa-10*$^{-/-}$*/Hoxd-11*$^{-/-}$ double mutants of both sexes are fully viable. The abnormalities described below were similar in 129/Sv inbred and 129/Sv-C57BL/6 hybrid genetic backgrounds. *Hoxa-10/Hoxd-11* double mutants of both sexes where hypofertile, to the same extent as previously described for *Hoxa-10*$^{-/-}$ male and female mutants (Satokata et al., 1995; Rijli et al., 1995), and for *Hoxd-11*$^{-/-}$ male mutants (Favier et al., 1995).

Neither *Hoxa-10*$^{-/-}$ nor *Hoxd-11*$^{-/-}$ single mutants (Favier et al., 1995) exhibited any external forelimb abnormality. In contrast, most of the double homozygous mutants and 25% of the *Hoxa-10*$^{+/-}$*/Hoxd-11*$^{-/-}$ mutants presented shortened and twisted forelimbs, with the forepaws turned outwards (data not shown). These malformations clearly impeded the animal motility, as judged by 'climbing tests' showing that control animals could hang themselves for more than 2 minutes to the cage cover grid, whereas mutant animals whose skeleton was the most affected could not hang for more than 10 seconds or not at all.

Double homozygous mutants exhibited severe alterations of the skeletal elements in the forelimb zeugopod, which were not seen in the single mutants. All *Hoxa-10*$^{-/-}$*/Hoxd-11*$^{-/-}$ mutants had shortened radius and ulna (20% shortening on average; Table 1, Fig. 5). However, the humerus and scapulae of the double mutants were not shortened, excluding a general growth deficiency (Table 1). Comparative measurements revealed that single *Hoxd-11*$^{-/-}$ mutants had a milder shortening of the radius and ulna (7 and 10%, Table 1) which was not reported in our initial study (Favier et al., 1995). In fact, the radius and ulna of *Hoxd-11*$^{-/-}$ mutants were morphologically normal, except in their distal extremities (Fig. 5B). In contrast, the radius and ulna of double homozygous mutants were truncated

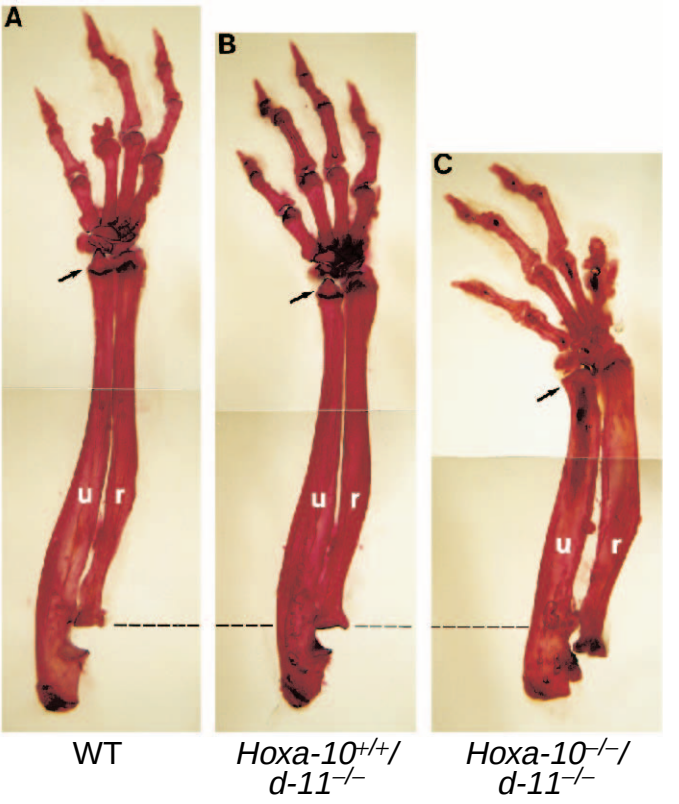

Fig. 5. Zeugopod alterations in *Hoxa-10*$^{-/-}$*/Hoxd-11*$^{-/-}$ mutants Dorsal views of the forelimb skeletons of a control (*Hoxa-10*$^{+/+}$*/Hoxd-11*$^{+/+}$) (A), a single *Hoxd-11*$^{-/-}$ mutant (B) and a double *Hoxa-10*$^{-/-}$*/Hoxd-11*$^{-/-}$ mutant specimen (C). Notice that the radius and ulna of the single mutant are slightly reduced but have a correct morphology. The same bones are strongly reduced and thickened, with an enlarged gap between them, in the double mutant. Notice the abnormal bending of the ulna distal extremity and the exaggerated angulation of the forefoot. Removal of the humerus induced a shift between ulna and radius in this preparation, so that the radius proximal extremity artefactually overlaps the articular surface of the ulna. r, radius; u, ulna.

Table 1. Limb phenotype

		Hox mutants					
	Control[a]	a10 -/- d11 wt	a10 wt d11 -/-	a10 +/- d11+/-	a10 -/- d11 +/-	a10 +/- d11 -/-	a10 -/- d11 -/-
Length reduction of limb bones[b]							
metacarpal 2	100%	96%	77%	100%	90%	73%	69%
metacarpal 3	100%	97%	83%	100%	88%	84%	79%
metacarpal 4	100%	97%	83%	100%	89%	85%	81%
phalange 1 of digit 2	100%	98%	83%	97%	84%	87%	81%
phalange 2 of digit 5	100%	107%	80%	97%	89%	83%	57%
radius	100%	95%	93%	98%	89%	95%	82%
ulna	100%	96%	90%	99%	89%	94%	79%
humerus	100%	98%	96%	104%	103%	100%	100%
scapula	100%	99%	93%	100%	99%	102%	98%
femur	100%	97%	94%	99%	98%	103%	97%
tibia	100%	96%	96%	99%	96%	100%	98%
Abnormalities[c]							
elbow sesamoid normal/altered[d]	34/0	10/0	26/0	14/0	12/0	26/6	15/11
d3 and c separated/fused	34/0	10/0	23/3	14/0	8/4	25/7	15/11
metacarpal sesamoid normal/altered[e]	31/3	10/0	18/8	8/6	9/3	24/8	21/5
ppsl fused/separated[f]	34/0	10/0	6/20	14/0	12/0	20/12	25/1
pyramidal and pisiform separated/fused[g]	34/0	10/0	1/25	14/0	12/0	6/26	0/26
ulna styloid normal/malformed[g]	34/0	10/0	0/26	14/0	8/4	0/32	0/26
absence/presence of sesamoids distal to ulna[g]	34/0	10/0	20/6	12/2	11/1	25/7	4/22

d3, distal carpal 3; c, central carpal bone, ppsl, palmar process of the scapholunate.

(a) Control include *Hoxa-10*$^{+/+}$ / *Hoxd-11*$^{+/+}$, *Hoxa-10*$^{+/-}$ / *Hoxd-11*$^{+/+}$ and *Hoxa-10*$^{+/+}$ / *Hoxd-11*$^{+/-}$ animals.

(b) Displayed as the % of the length of the same bone in control littermate specimen. Mean values for each genotype were calculated out of 5-7 animals each. Metacarpal 5 and other phalanges were less reduced (>90% of normal length) in all mutant genotypes, and are not displayed in this table.

(c) Number of limbs with normal / abnormal morphology.

(d) Include an extra or a bigger than usual lateral sesamoid bone or a medial one (found in three double mutant limbs) or combination.

(e) Bigger sesamoid at the palmar and proximal end of the fourth metacarpal and/or presence of extra sesamoid bones at the palmar and proximal end of the third and/or the second metacarpal.

(f) In *Hoxa-10*$^{+/-}$ / *Hoxd-11*$^{-/-}$ and in *Hoxa-10*$^{-/-}$ / *Hoxd-11*$^{-/-}$ mutant limbs, when the ppsl is fused to the scapholunate, it often (~50%) presents evidence of secondary or even incomplete fusion to the main bone, which is not observed in control limbs.

(g) See Figs 7 and 8 for details. No distinction is made in this table regarding the extent of the malformations.

and thicker (Fig. 5C). The abnormal angularity of the forepaw skeleton (compare Fig. 5C to A,B) probably results from both a greater size reduction of the ulna and a severe alteration of its styloid apophysis (see below).

The proximal region of the ulna was not clearly altered in single *Hoxd-11*$^{-/-}$ mutants (Fig. 7B), but was severely affected in some double mutants, with extra bone ridges at the insertion site of the triceps brachialis and biceps brachialis muscles and an apparent truncation of the olecranion (Figs 7C, 5C). Several double mutants also had extra sesamoid bones or alterations of the shape of the normal elbow sesamoid (data not shown; Table 1).

The additional homozygous disruption of *Hoxa-10* also increased the severity of the *Hoxd-11*$^{-/-}$ autopod alterations. As previously described (Davis and Capecchi, 1994; Favier et al., 1995), *Hoxd-11*$^{-/-}$ mutants display variable archipodium abnormalities which include slight alterations of the ulna and radius styloids, pisiform/pyramidal and/or pyramidal/scapholunate bone fusions, truncation of the pisiform bone, separation of the palmar process of the scapholunatum and occasional supernumerary sesamoids. The neopodium abnormalities essentially consist of size reductions of metacarpals II to V and of the second phalanx of digit II. In newborn double homozygous mutants, the autopod appeared similar to those of single *Hoxd-11*$^{-/-}$ mutants (Favier et al., 1995) with a additional minor alteration of the pyramidal. The radius and ulna were only slightly reduced, and the ulna styloid appeared normal. The percentage reduction increased by 3 and 6 days post-partum and at the same time a gap appeared between the ulna styloid and the pyramidal bone (data not shown). In adults, the ulna styloid was much more severely truncated in *Hoxa-10*$^{-/-}$/*Hoxd-11*$^{-/-}$ mutants (Figs 6B,C, 7F) than in single *Hoxd-11*$^{-/-}$ mutants (Fig. 7E). Thus, there was no articular relationship between the ulna styloid and pyramidal bone (compare Fig. 6A to B,C). Some extra sesamoid bones were often present dorsally (Fig. 6B, brace) or laterally (Fig. 6C, thin arrow) to the pyramidal bone. These may result from an induced instability of the wrist (Fig. 6B, brace), or may represent unfused vestigia of the ulna styloid (Fig. 6C, thin arrow). Some double mutants also presented a wide gap (Fig. 6C, large arrow), sometimes associated with an abnormal excrescence (Figs 6B, 7F, black arrows) at the radial side of the ulna. By contrast, the distal extremity of the radius was not more malformed than in *Hoxd-11*$^{-/-}$ single mutants (Fig. 6B,C, white open arrows). The severity of the *Hoxd-11*$^{-/-}$ alterations of the pyramidal and pisiform bones (the two posterior bones of the proximal row of the carpus) was also increased in double mutants. Not only were these bones always fused in the *Hoxa-10*$^{-/-}$/*Hoxd-11*$^{-/-}$ mutants, but they were more truncated than in the single *Hoxd-11*$^{-/-}$ mutants (compare Fig. 7H and I). Additional differences between the carpal alterations of double and single mutants included: (i) a reduced rate of fusion between the scapholunate and the pyramidal bone, (ii) an enlargement of the sesamoid bone at the palmar base of metacarpal 4 and/or extra sesamoids at the base of other metacarpals, (iii) a reduced rate

of separation of the palmar process of the scapholunate, (iv) a fusion between the central and distal three carpal bones (Table 1). This latter abnormality was also found in some *Hoxd-11*$^{-/-}$ single mutant littermates; a foundator effect may explain why this fusion was not seen in our previous study (Favier et al., 1995).

The size reduction of metacarpals II and, to a lesser extent of metacarpals III and IV, was also more pronounced in double homozygous mutants than in single *Hoxd-11*$^{-/-}$ mutants (Table 1). Interestingly, the second phalanx of digit V of double mutants was both truncated and malformed, which was not observed in single *Hoxd-11*$^{-/-}$ mutants (not shown).

The *Hoxa-10*$^{+/-}$*/Hoxd-11*$^{-/-}$ mutants displayed variable forelimb abnormalities. Whereas some mutants had malformations similar to those of *Hoxd-11*$^{-/-}$ single mutants, others exhibited wrist alterations which were as severe as in double homozygous mutants (data not shown). In contrast, *Hoxa-10*$^{-/-}$*/Hoxd-11*$^{+/-}$ mutants had no forelimb abnormalities, except for the presence of a small sesamoid bone between the radius and the pisiform (already seen in some *Hoxd-11*$^{+/-}$ mutants, Favier et al., 95) and, in some mutants, there were a mild alteration of the ulna styloid and slight size reductions of the ulna, radius and some metacarpal and phalangeal elements (data not shown; see Table 1).

The hindlimb phenotype of *Hoxa-10*$^{-/-}$*/Hoxd-11*$^{-/-}$ double mutants was indistinguishable from that of single *Hoxa-10*$^{-/-}$ mutants. We did not detect size or shape alterations of the tibia, fibula or of any other hindfoot elements (data not shown; see Table 1).

Increased penetrance of the vertebral transformations in *Hoxa-10/Hoxd-11* double mutants

Wild-type (WT) mice have 7 cervical, 13 thoracic, 6 lumbar, 4 sacral and a variable number of caudal (Ca) vertebrae (7C,13T,6L,4S phenotype). As previously reported, about half of the *Hoxd-11*$^{-/-}$ mutants have 7 lumbar vertebrae (7C,13T,7L,4S phenotype), indicating that vertebra #27 was transformed from a S1 to a 'L6-like' morphology, all subsequent vertebrae being anteriorly transformed at least until vertebra #32 (Ca2, transformed into a Ca1* vertebra) (Favier et al., 1995; Fig. 8). Furthermore, in most of *Hoxd-11*$^{-/-}$ animals with 7 lumbar vertebrae, vertebra #25 (WT L5) had the accessory processes characteristic of an L4 identity (see Materials and methods), while spinous and lateral processes of vertebrae #25, #26 and #27 were similar to those of WT L4, L5 and L6 vertebrae, respectively (Fig. 8).

The *Hoxd-11*$^{-/-}$*/Hoxa-10*$^{+/-}$ mutants showed the same altered phenotype as single *Hoxd-11*$^{-/-}$ mutants, but with a full penetrance: 15 out of 16 skeletons had seven lumbar vertebrae and the #27 vertebra of the last specimen was partially transformed from a S1 to a lumbar morphology; using the criteria described in Materials and methods, all vertebrae #25, #26 and #27 were anteriorly transformed (L4*, L5*, L6* in Fig. 8).

Most *Hoxa-10*$^{-/-}$ mutants have a 7C,14T,5L,4S phenotype, vertebra #21 being transformed from a L1 to a 'T13-like' morphology. These anterior transformations always extend down to vertebra #24 (L4 transformed into L3*) and, with an incomplete (50%) penetrance, down to vertebra #26 (L5 and L6 transformed into L4* and L5*) (Rijli et al., 1995). We noticed that in 4 out of 34 mutants, vertebrae #27 and #28 were also transformed (S1 and S2 transformed into L6* and S1*, these mutants having a 7C,14T,6L,3S phenotype). No increase in penetrance or expressivity of the *Hoxa-10*$^{-/-}$ thoracic transformations (Rijli et al., 1995) was detected in any *Hoxd-11/Hoxa-10* double mutants. All but two *Hoxa-10*$^{-/-}$*/Hoxd-11*$^{+/-}$ mutants displayed anterior transformations from vertebra #21 to #32 (Fig. 8). One specimen displayed anterior transformations from vertebrae #21 to #26 only (as some single *Hoxa-10*$^{-/-}$ mutants) and another from vertebrae #21 to #28 (as the most affected single *Hoxa-10*$^{-/-}$ mutants). Thus, *Hoxa-10*$^{-/-}$*/Hoxd-11*$^{+/-}$ mutants exhibited transformations which were at least those of single *Hoxa-10*$^{-/-}$ mutants, but more frequently encompassed the domain of anterior transformation of both *Hoxa-10* and *Hoxd-11* mutations (Fig. 8). Note that heterozygous *Hoxd-11*$^{+/-}$ mutants did not display any axial skeleton abnormalities in this region.

All *Hoxa-10*$^{-/-}$*/Hoxd-11*$^{-/-}$ mutants had a 7C,14T,6L,4S phenotype. Vertebrae #21 to #32 were anteriorly transformed as if the affected region would result from the reunion of the *Hoxa-10*$^{-/-}$ and the *Hoxd-11*$^{-/-}$ ones, but with a full penetrance (Fig. 8). Moreover, the accessory processes of vertebra #26 displayed an L4-like morphology in 10/13 cases. This could be considered as a partial anterior transformation of a L6 to L4 morphology (L4** in Fig. 8). In about 50% of the double homozygous mutants, and one *Hoxa-10*$^{-/-}$*/Hoxd-11*$^{+/-}$ mutant, we found one abnormal posterior lumbar vertebra (#25, #26 or #27) which could not be easily ranked; these vertebrae were assigned a rank between those of its two neighbours.

Both *Hoxd-11*$^{-/-}$ and *Hoxa-10*$^{-/-}$ single mutants inconsistently showed abnormal fusions between spinous processes of two sacral vertebrae, S2 and S3, whether the sacrum was at its normal position (S2 and S3 are vertebrae #28 and #29) or was composed of anteriorly transformed vertebrae [S2* and S3* are then vertebrae #29 and #30, see Fig. 8, footnote (e)]. These fusions were consistently found in the *Hoxa-10*$^{-/-}$*/Hoxd-11*$^{+/-}$ and *Hoxa-10*$^{-/-}$*/Hoxd-11*$^{-/-}$ mutants; in three of the double homozygous mutants, we even found fusion of three sacral spinous processes.

Taken together and in spite of some variability in the lumbosacral vertebral phenotype for a given genotype (higher in mutant than in control animals), our data indicate extensive anterior transformation of the lumbar and sacral vertebrae, with a maximum penetrance in the double mutants.

DISCUSSION

The *Hoxa-10*$^{-/-}$ mutation selectively affects structures of the hindlimb stylopod

The alterations detected in *Hoxa-10*$^{-/-}$ mutants are essentially limited to the hindlimbs, even though *Hoxa-10* displays similar expression patterns in the developing forelimbs and hindlimbs. These hindlimb alterations are restricted to a proximal region which encompasses the stylopod and the knee region, but excludes the femoral head, thus extending proximally up to the developmental expression boundary of *Hoxa-10*. The subtle and inconsistent alterations of the humeral deltoid crest may represent a mild counterpart of the hindlimb third trochanter abnormalities. In contrast, the *Hoxd-11* mutation affects a limited region of the forelimb autopod, with only minor effects in hindlimbs (Davis and Capecchi, 1994; Favier et al., 1995), and *Hoxa-9/Hoxd-9* double mutations also selectively affect

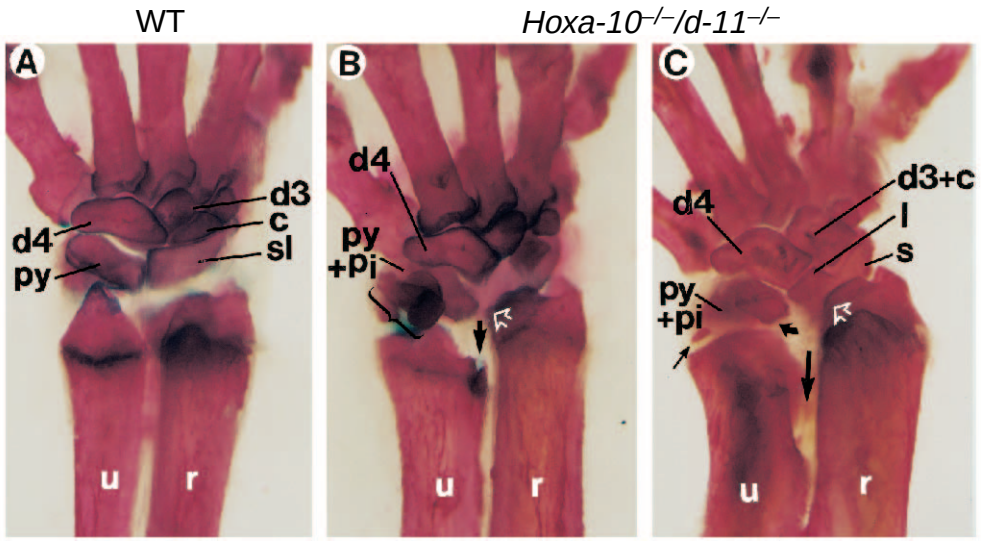

Fig. 6. Carpal alterations in *Hoxa-10$^{-/-}$/Hoxd-11$^{-/-}$* mutants. Dorsal views of the carpus of a WT animal (A) and two *Hoxa-10$^{-/-}$/Hoxd-11$^{-/-}$* mutants (B,C). The mutant ulna styloids are severely truncated, especially in C. Note that the radius styloid is only slightly affected at its ulnar side (white open arrows), as seen in *Hoxd-11$^{-/-}$* single mutants. (B), The thick arrow indicates an abnormal excrescence at the ulna extremity (see also Fig. 7F). The pyramidal is partly hidden by a de novo large sesamoid bone (brace) which is in continuity with extensor muscle tendons. (C) The distal extremity of the ulna is abnormally bent, generating a central gap (large arrow). The curved arrow indicates a truncated polygonal portion of the pyramidal bone which lies at the same level, but has no articular relationship with the scapholunate bone, the os hamatum and the ulna styloid. The small arrow points to a small bone that may correspond to an unfused vestigia of the ulna styloid. Note also the fusion between the central bone and the distal carpal 3 and the altered shape of the scapholunate, typical of some *Hoxd-11$^{-/-}$* single mutants. c, os centrale; d3, os capitatum or distal carpal 3; d4, os hamatum or distal carpals 4/5; l, lunate portion of the scapholunate; r, radius; s, scaphoid portion of the scapholunate; sl, scapholunate; py, os triquetrum or pyramidal; py+pi, fused pyramidal and pisiform bones; u, ulna.

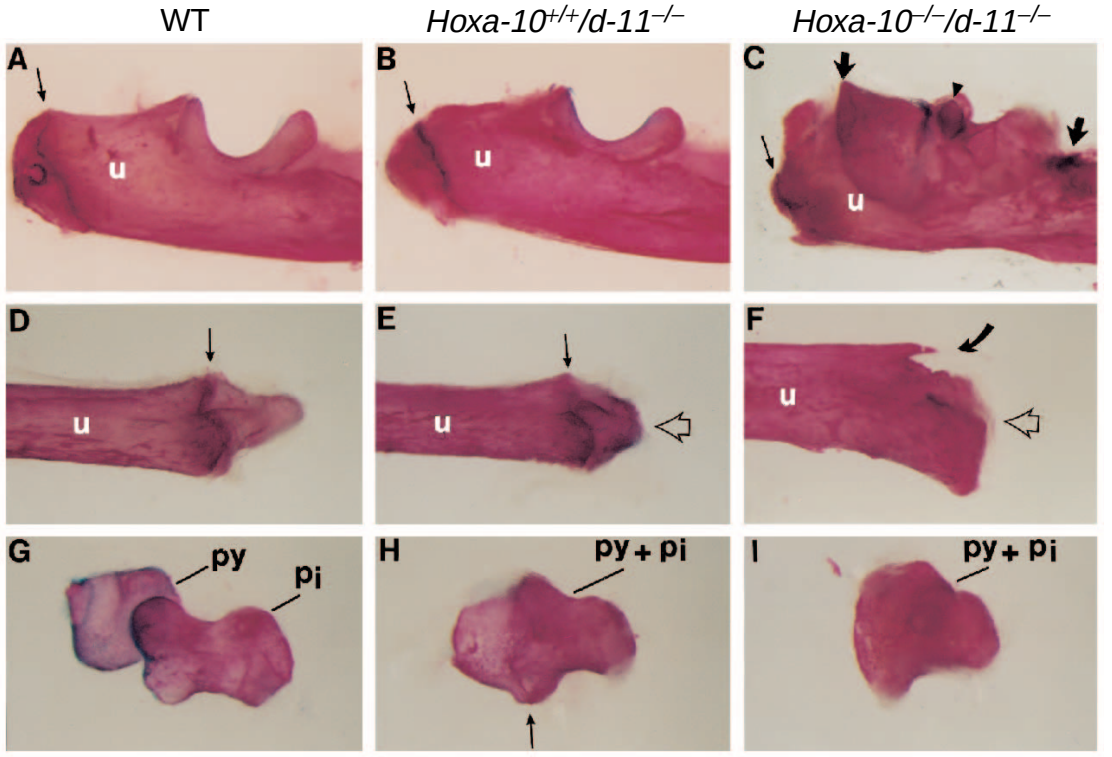

Fig. 7. Details of the forelimb skeleton in WT animals (A,D,G), single *Hoxd-11$^{-/-}$* (B,E,H) and double *Hoxa-10$^{-/-}$/Hoxd-11$^{-/-}$* (C,F,I) mutants. (A-C) Proximal portion of the ulna, medial views. The olecranion (*tuber olecrani*) is only slightly affected in the simple *Hoxd-11$^{-/-}$* mutant (B). The thin arrow points to the fusion line between the diaphysis and the part derived from the proximal ossification center. (C) The olecranion and the entire articular region are strongly misshapen in this double *Hoxa-10$^{-/-}$/Hoxd-11$^{-/-}$* mutant and the fusion line cannot easily be identified. The thin arrow tentatively indicates such a line. The large arrows indicate abnormal ridges which were connected to the triceps brachialis, ancone and biceps brachialis muscle tendons before dissection. The arrowhead points to an abnormal process close to the articular surface. (D-F) Distal extremity and styloid of the ulna, dorsal views. The styloid of the single *Hoxd-11$^{-/-}$* mutant (E) is mildly truncated with a round shape (open arrow). The distal aspect of the *Hoxa-10$^{-/-}$/Hoxd-11$^{-/-}$* ulna (F, open arrow) is almost flat. The styloid is difficult to recognize as there is no fusion line of its secondary ossification center (thin arrows in D and E). The curved arrow shows an abnormal process at the radial side of the ulna extremity. (G-I) Dissected pyramidal and pisiform bones, lateral views. Dorsal side is to the left, palmar side to the right. The pyramidal and pisiform of the single *Hoxd-11$^{-/-}$* mutant (H) are fused and truncated, but the line of fusion is recognizable (thin arrow) and the pisiform still has a typical shape. In the double *Hoxa-10$^{-/-}$/Hoxd-11$^{-/-}$* mutant (I), the line of fusion cannot be identified and the pisiform part is severely truncated. pi, pisiform; py, pyramidal; py+pi, fused pyramidal and pisiform bones; u, ulna.

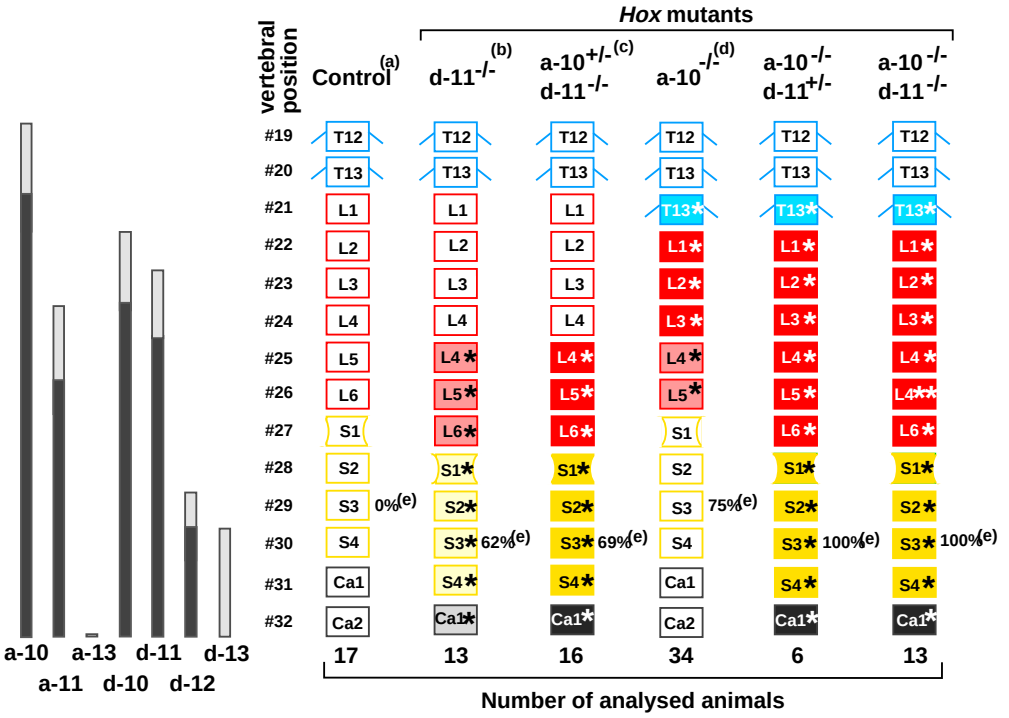

Fig. 8. Schematic representation of the lumbar and sacral vertebral transformations of *Hoxa-10* and *Hoxd-11* single and compound mutants. Thoracic vertebrae (T) are in blue, lumbar (L) in red, sacral (S) in yellow and caudal (Ca) in black. The transformed vertebrae are filled according to the penetrance of the transformation: light shading indicates a 30-80% penetrance, and full color a 90-100% penetrance. The thoracic transformations found in *Hoxa-10* mutants are not represented. The bars on the left indicate the expression domain of 'posterior' *Hoxa* and *Hoxd* genes in the developing vertebral column, light grey indicating lower levels of expression. (a) Control animals were taken from the following genotypes: WT and single *Hoxa-10*$^{+/-}$ or *Hoxd-11*$^{+/-}$ heterozygous animals. No skeleton from other genotypes was analyzed without at least one control animal from the same litter, analysed at the age of 3-4 months. (b) This phenotype is not fully penetrant (Favier et al., 95). In the series analyzed in this study, 6/13 skeletons were normal and one presented an asymmetrical transformation of vertebra #26. The six remaining specimens had 7 lumbars, the anterior transformation extending to #25 (which acquired the L4 morphological criteria described hereabove). (c) *Hoxd-11*$^{-/-}$/*Hoxa-10*$^{+/-}$ displayed the same phenotype as *Hoxd-11*$^{-/-}$/*Hoxa-10*$^{+/+}$ mutants, but with a nearly full penetrance. Only one skeleton displayed a #27 vertebra with an intermediate morphology between S1 and L6. (d) In most *Hoxd-11*$^{+/+}$/*Hoxa-10*$^{-/-}$ mutants, the anterior transformation (Rijli et al., 1995) occurred as illustrated down to vertebra #26, but occasionally extended down to #29 (which acquired an intermediate S2-S3 morphology) in 12% of the specimen. (e) This is the percentage of skeletons with abnormal fusion (no fusion was observed in control skeletons) between the spinous processes of two sacral vertebrae, usually S2 and S3 (or S2* and S3*). In three *Hoxd-11*$^{-/-}$/*Hoxa-10*$^{-/-}$ mutants, a third spinous process (of S1* or S4*) was involved.

the skeleton of the forelimb stylopod (Fromental-Ramain et al., 1996). The almost complete lack of forelimb alterations in *Hoxa-10*$^{-/-}$ mutants cannot be readily accounted for by functional redundancies between *Hoxa-10* and its paralogous genes, since *Hoxd-10* is not expressed as proximally as *Hoxa-10* (our unpublished data) and *Hoxc-10* is apparently not expressed in the forelimb mesenchyme (Peterson et al., 1995). It is therefore likely that, if *Hoxa-10* plays a role in the development of the forelimb stylopod, its inactivation can be functionally compensated by more 3′-located *Hox* genes, e.g. *Hoxa-9* and *Hoxd-9* (see Fromental-Ramain et al., 1996 for further discussion of this point).

Whereas the *Hox* mutant limb phenotypes previously reported (Dollé et al., 1993; Small and Potter, 1993; Davis and Capecchi, 1994; Favier et al., 1995) correspond to bone truncations and fusions, i.e. to the lack of skeletal material, the present *Hoxa-10* femoral phenotype is characterized by the presence of extra skeletal material along the lateral side (labium laterale) of the femur. The enlarged third trochanter may represent a primary effect of the *Hoxa-10*$^{-/-}$ mutation, since it correlates with a preferential expression of *Hoxa-10* during fetal stages (13.5-14.5 dpc) around a portion of the differentiating femur. The lack of *Hoxa-10* expression at these stages may alter the local production or recruitment of cells with a skeletogenic fate. We believe that the supernumerary 'ligament', which links the third trochanter to the lateral condyle, rather than being a de novo structure, is a thickening of the septum intermuscularis femoris lateralis. This 'ligament' has indeed the same anatomical relationships as the WT septum, including a histological continuity with the periosteum. The merging of part of the gluteus superficialis tendon in the mutant 'ligament' reflects the WT situation in which this tendon is in continuity with the septum and the fascia lata at its site of insertion. The abnormal thickening might be the consequence of antagonistic tensions between the gastrocnemius and the gluteus superficialis which is misplaced on the mutant third trochanter. The altered shape of the lateral knee sesamoid may in turn be a consequence of such mechanistic phenomena, since sesamoid bone morphologies are known to depend on pressure stress in connective structures during fetal development (Hall, 1986; Hinchliffe, 1994). However, two alternative possibilities cannot be ruled out. Firstly, the 'ligament' might derive from a distal subset of the cells which are abnormally recruited proximally to form the altered third trochanter. Secondly, an abnormal patterning of the gluteus superficialis muscle, or at least of its distal insertion, might be a primary effect of the *Hoxa-10*$^{-/-}$ mutation. The expression of *Hoxa-10* in presumptive limb muscle cells (Haack and Gruss, 1993) and in the femur periosteum at 14.5 dpc (this study) may support this hypothesis. Thus the primary effect of the *Hoxa-10*

mutation remains elusive, since the abnormal 'ligament', third trochanter and gluteus superficialis muscle insertion appear to synergistically produce the mutant phenotype.

Partial functional redundancy between *Hoxa-10* and *Hoxd-11* in forelimb morphogenesis

Although *Hoxa-10* is expressed in the developing forelimb, its inactivation generates almost no skeletal abnormalities. In contrast, *Hoxd-11* inactivation affects a restricted skeletal region of the forelimb autopod, essentially the proximal row of the carpus and some metacarpal bones (Davis and Capecchi, 1994; Favier et al., 1995). Interestingly, *Hoxa-10*$^{-/-}$/*Hoxd-11*$^{-/-}$ mutants exhibit a 'synergistic' forelimb phenotype, characterized by alterations which are milder in the *Hoxd-11*$^{-/-}$ mutants, such as the truncations of the ulna styloid, pisiform and pyramidal bones, metacarpal bones and second phalanx of digit V. In addition, there are striking alterations in a more proximal region nearly unaffected in single *Hoxd-11*$^{-/-}$ mutants which display only a subtle shortening of the radius and ulna. These alterations, which extend up to the most proximal expression domain of *Hoxd-11* in the developing zeugopod, correspond to truncations and thickening of the radius and ulna, and deformations of the ulna proximal articular surface. As for the metacarpal bones in single *Hoxd-11*$^{-/-}$ mutants (Favier et al., 1995), these alterations appear only after birth. Further studies are necessary to investigate whether these late arising defects reflect a direct effect of *Hoxa-10* or *Hoxd-11* after birth or the consequences of underlying defects occurring prior to birth.

Thus, *Hoxa-10* can exert a morphogenetic function in regions that are not affected in single *Hoxa-10*$^{-/-}$ mutants. Clearly, two non-paralogous *Hox* genes which are co-expressed in the developing zeugopod and autopod of the forelimb can have partly redundant functions, which are revealed only upon inactivation of both genes. Furthermore, there is a gene dosage effect, as *Hoxa-10*$^{+/-}$/*Hoxd-11*$^{-/-}$ mutants display features of the double homozygous mutant phenotype, albeit with a lower penetrance. However, *Hoxa-10* or *Hoxd-11* are not functionally equivalent as *Hoxa-10*$^{-/-}$/*Hoxd-11*$^{+/-}$ mutants display almost no forelimb abnormalities, except for slight bone size reductions. Thus, *Hoxd-11* appears to be more critical than *Hoxa-10* for zeugopodal and autopodal forelimb morphogenesis. Part of the more severe 'double mutant' carpal phenotype might develop as a consequence of the malformations in the zeugopod: the truncation of the ulna primordium may generate a post-axial gap in the developing carpus, such that the pyramidal primordium would lose its relationship with other elements except the pisiform. This could explain why, in double mutants, the pyramidal displays no recognisable articular surface and is systematically fused to the pisiform, but not to the scapholunate. The abundance of extra sesamoids may be a consequence of the instability of the wrist articulation, generating abnormal tensions in the wrist extensor and digit flexor muscle tendons.

Davis et al. (1995) have proposed a model of *Hox* gene function in limb development in which each paralogous *Hox* group 9 to 13 would specify, respectively, the scapulum, stylopodal, zeugopodal, archipodium autopodal and neopodium autopodal bones. The *Hoxa-10*$^{-/-}$ hindlimb phenotype is in agreement with this proposal, which, however, did not predict that *Hoxa-10* can be functional in the developing ulna and radius (zeugopod), as shown in the present study (at least in a *Hoxd-11*$^{-/-}$ background). Davis et al. (1995) also proposed that the metacarpal and phalangeal neopodium alterations seen in *Hoxd-11*$^{-/-}$ mutants were secondary to the patterning defects of the zeugopod. We rather believe that the neopodium abnormalities seen in *Hoxd-11*$^{-/-}$ and *Hoxa-10*$^{-/-}$/*Hoxd-11*$^{-/-}$ mutants reflect a primary morphological function (and not a secondary consequence of the more proximal phenotype) of *Hoxd-11* and *Hoxa-10* in this region for the following reasons: (i) the neopodium is a tetrapod neomorphic structure (Shubin and Alberch, 1986; Sordino et al., 1995), (ii) *Hoxd-11* has two domains of expression in mouse limb buds, one of which corresponds to the neopodium (Sordino et al., 1995; Davis and Capecchi, 1994), (iii) the autopodal structures are differently affected by the *Hoxa-10/Hoxd-11* mutations (The second carpal row is mainly unaffected and the metacarpals are more affected than most phalanges).

There is no synergistic effect of the double *Hoxa-10*$^{-/-}$/*Hoxd-11*$^{-/-}$ mutation on the generation of hindlimbs abnormalities. This further demonstrates that *Hox* genes, even though they are expressed in both limbs, may act differently during forelimb and hindlimb development. This lack of a synergistic effect between *Hoxa-10*$^{-/-}$ and *Hoxd-11*$^{-/-}$ mutations in the hindlimbs may reflect a functional redundancy of *Hoxc-9, Hoxc-10 or Hoxc-11*, which are expressed in the hindlimb, but not the forelimb mesenchyme (Peterson et al., 1994).

Taken together, our results demonstrate that during limb development: (i) a given *Hox* gene can act in a 'specific' domain (here *Hoxd-11* in the autopod), where its function cannot be fulfilled by other *Hox* genes, and (ii) it can also act in a wider 'redundant' domain where the loss of its function can be compensated for by (an)other *Hox* gene product(s) (here *Hoxa-10*). There are several examples of functional redundancy between *Hox* paralogues during limb development: *Hoxa-9* and *Hoxd-9* in the developing forelimb stylopod (Fromental-Ramain et al., 1996), *Hoxa-11* and *Hoxd-11* in the forelimb zeugopod (Davis et al., 1995), and *Hoxa-13* and *Hoxd-13* in both limb autopods (our unpublished results). Importantly, we show here that functional redundancy exists even between non-paralogous genes which are co-expressed in a given region of the developing limbs, i.e. *Hoxa-10* and *Hoxd-11* in the forelimb zeugopod. Thus, in disagreement with a strict application of the posterior prevalence principle (Duboule, 1991, but see also Duboule and Morata, 1994), functional redundancy is not limited to members of the same paralogous group, and a given *Hox* gene can specify structures in a region where it is co-expressed with more 5′-located non-paralogous genes. However, one should stress in this respect that the functional redundancy which is revealed by the comparison of the phenotypes of single and double mutants may not reflect the physiological situation: the knock-out of a physiologically relevant *Hox* gene may create a new situation in which other paralogous or non-paralogous *Hox* gene(s) expressed in the same region, could 'artefactually' replace the relevant gene. In other words, genes that appear to be functionally redundant from knock-out studies may not be redundant in normal development (see also Fromental-Ramain et al., 1996).

Cooperation between non-paralogous *Hox* genes for vertebra specification

In the developing prevertebral column, the two non-paralogous

genes *Hoxa-10* and *Hoxd-11* are widely co-expressed caudally to prevertebra #24, while only *Hoxa-10* is expressed in more anterior regions up to prevertebra #21. As expected from its expression domain, our results show that *Hoxd-11* has no effect alone or in combination with *Hoxa-10*, rostral to vertebra #25, where the same phenotype of anterior transformations of vertebrae #21 to #24 is seen in *Hoxa-10*$^{-/-}$, *Hoxa-10*$^{-/-}$*/Hoxd-11*$^{+/-}$ and *Hoxa-10*$^{-/-}$*/Hoxd-11*$^{-/-}$ mutants (see Fig. 8).

Interestingly, the anterior transformation of vertebrae #25 and #26 becomes fully penetrant in *Hoxa-10*$^{-/-}$*/Hoxd-11*$^{+/-}$ and in *Hoxa-10*$^{+/-}$*/Hoxd-11*$^{-/-}$ double mutants, whereas it is only partially penetrant in *Hoxa-10*$^{-/-}$ and in *Hoxd-11*$^{-/-}$ single mutants. Thus, two non-paralogous genes belonging to different *HOX* complexes appear to be partially redundant for the specification of vertebrae #25 and #26. Whether this cooperation corresponds to a 'quantitative' effect (both gene products triggering the same molecular events) or to a 'qualitative' effect, (each gene product triggering distinct 'parallel' events which are not absolutely required on their own) is unknown. We note that the present functional cooperation between two non-paralogous genes is reminiscent of that reported for *Hoxb-5* and *Hoxb-6*, where *Hoxb-5*$^{+/-}$*/Hoxb-6*$^{+/-}$ transheterozygotes display a malformation also present in either single homozygote mutants (Rancourt et al., 1994). In any event, the *Hoxa-10/Hoxd-11* functional cooperation is compatible with a combinatorial model of vertebra specification by at least some of the *Hox* genes which are expressed in a given prevertebral segment (Kessel and Gruss, 1991). The fact that *Hoxd-11*$^{-/-}$ mice exhibit with a partial penetrance an anterior transformation of vertebrae #29-#32, even though *Hoxd-11* is coexpressed in this region with *Hoxd-12* and *Hoxd-13* (see Fig. 8) further support a combinatorial model. Similarly, the observations that all vertebrae #27 to #32 were anteriorly transformed with a full penetrance in *Hoxa-10*$^{+/-}$*/Hoxd-11*$^{-/-}$, *Hoxa-10*$^{-/-}$*/Hoxd-11*$^{+/-}$ and *Hoxa-10*$^{-/-}$*/Hoxd-11*$^{-/-}$ are in agreement with a combinatorial model.

In all cases, the above partial functional redundancies between non-paralogous genes are inconsistent with the posterior prevalence model as initially formulated for limb development (Duboule, 1991), since this model stipulates that a given *Hox* gene would specify structures only in the region where there is no more posterior (5′-located) *Hox* gene expressed. This rule also postulates that "anterior structures would be produced by default, i.e. as a result of the non-expression of more posterior genes". The present anterior transformations are in agreement with this proposal. However, it is noteworthy that, in view of the expression domains of the *Hoxd* genes (see Fig. 8), one might have expected to see all vertebrae #25 to #29 acquiring a L4 identity, which is clearly not the case. As argued by Duboule and Morata (1994), the interpretation of the effects of *Hox* gene loss-of-function mutation is made more difficult in vertebrates than in *Drosophila*, due to (i) the existence of paralogous genes, (ii) quantitative aspects of the posterior prevalence rule which are apparent even in *Drosophila*, and (iii) possible perturbing effects of the mutation on cross-regulation between *Hox* genes. The disruption of all genes whose anterior boundary of expression is posterior to vertebra #24 (including *Hoxd-11*) may be required to see all more posterior vertebrae acquiring an L4 identity. In this respect, we note that vertebrae #26 is converted from an L6 identity in WT to a L4 identity in *Hoxa-10*$^{-/-}$*/Hoxd-11*$^{-/-}$ double mutants.

Finally, it is striking that the anterior transformations of all vertebrae #25 to #32 are 50% penetrant in *Hoxd-11*$^{-/-}$ mutants and 100% penetrant in the *Hoxd-10*$^{+/-}$*/Hoxd-11*$^{-/-}$ double mutants. Even a 'quantitative' functional prevalence (Duboule and Morata, 1994) of *Hoxd-12* and *Hoxd-13* would require that the penetrance of the *Hoxd-11* mutation decreases in the vertebrae #29-#32 region, where *Hoxd-12* and *Hoxd-13* are expressed. However we note that the penetrance of the anterior transformations decreases in *Hoxa-10*$^{-/-}$ mutants caudal to vertebrae #25 where *Hoxa-11* and *Hoxd-11* are co-expressed. Thus, either there is no 'quantitative' functional prevalence of *Hoxd-12* and *Hoxd-13* over *Hoxd-11*, or one may speculate that the *Hoxd-11* mutation generates a real duplication of vertebra #25 with a concomitant 'reranking' of the following vertebrae during their successive specification. This would assume that there is a recurrent mechanism for specification of vertebrae, which does not specify the identity of a given vertebra according to its absolute position, but rather according to the specification of its neighbour. Such a spatiotemporal control, which might be exerted at an early time during gastrulation, would of course make the interpretation of the axial skeleton phenotypes resulting from *Hox* gene loss-of-function mutations more difficult.

We thank S. Ward for a critical reading of the manuscript, R. Matyas for dissection of *Hoxa-10* mutant mice, M. Gendron, A. Sourine and M. LeMeur for the animal facilities, and M. Poulet for technical help. This work was supported by funds from the Institut National de la Santé et de la Recherche Médicale, the Centre National de la Recherche Scientifique, the Centre Hospitalier Universitaire Régional, the Association pour la Recherche sur le Cancer (ARC), and the Fondation pour la Recherche Médicale (FRM). B. F. was supported by a fellowship from La Ligue Nationale contre le Cancer, and F. M. R. by a fellowship from the ARC and the Université Louis Pasteur, Strasbourg.

REFERENCES

Barone, R. (1986). *Anatomie Comparée des Mammifères Domestiques.* 3rd Ed. Paris: Vigot Freres.

Davis, A. P. and Capecchi, M. R. (1994). Axial homeosis and appendicular skeleton defects in mice with a targeted disruption of *Hoxd-11*. *Development* **120**, 2187-2198.

Davis A. P., Witte, D. P., Hsieh-Li H. M., Potter, S. S. and Capecchi M. R. (1995). Absence of radius and ulna in mice lacking *Hoxa-11* and *Hoxd-11*. *Nature* 375, 791-795.

Dollé, P., Izpisúa-Belmonte, J. C., Falkenstein, H., Renucci, A. and Duboule, D. (1989). Coordinate expression of the murine *Hox-5* complex homeobox-containing genes during limb pattern formation. *Nature* **342**, 767-772.

Dollé, P., Dierich, A., LeMeur, M., Schimmang, T., Schuhbaur, B., Chambon, P. and Duboule, D. (1993). Disruption of the *Hoxd-13* gene induces localized heterochrony leading to mice with neotenic limbs. *Cell* **75**, 431-441.

Duboule, D. (1991). Patterning in the vertebrate limb. *Curr. Opin. Genet. Dev* **1**, 211-216.

Duboule, D. (1992). The vertebrate limb: a model system to study the *HOX/HOM* gene network during development and evolution. *BioEssays* **14**, 375-384.

Duboule, D. and Dollé, P. (1989) The structural and functional organization of the murine *HOX* gene family ressembles that of *Drosophila* homeotic genes. *EMBO J.* **8**, 1497-1505.

Duboule, D. and Morata, G. (1994). Colinearity and functional hierarchy among genes of the homeotic complexes. *Trends Genet.* **10**, 358-364.

Favier, B., LeMeur, M., Chambon, P. and Dollé, P. (1995). Axial skeleton homeosis and forelimb malformations in *Hoxd-11* mutant mice. *Proc. Natl. Acad. Sci. USA* **92**, 310-314.

Fromental-Ramain, C. Warot, X., Lakkaraju, S. Favier, B., Haack, H., Birling, C., Dierich, A., Dollé, P. and Chambon, P. (1996). Specific and redundant functions of the paralogous *Hoxa-9* and *Hoxd-9* genes in forelimb and axial skeleton patterning. *Development* **122**, 461-472.

Haack, H. and Gruss, P. (1993). The establishment of murine *Hox-1* expression domains during patterning of the limb. *Dev. Biol.* **157**, 410-422.

Hall, B. K. (1986). The role of movement and tissue interactions in the development and growth of bone and secondary cartilage in the clavicle of the embryonic chick. *J. Embryol. Exp. Morph.* **93**, 133-152.

Hinchliffe, J. R. (1994). Evolutionary developmental biology of the tetrapod limb. *Development* **1994 Supplement**, 163-168.

Izpisúa-Belmonte, J.-C., H. Falkenstein, P. Dollé, A. Renucci and D. Duboule. (1991) Murine genes related to the Drosophila *Abd B* homeotic gene are sequentially expressed during development of the posterior part of the body. *EMBO J.* **10,** 2279-2289.

Kessel, M., and Gruss, P. (1991). Homeotic transformations of murine vertebrae and concomitant alteration of *Hox* codes induced by retinoic acid. *Cell* **67**, 89-104.

Peterson, R. L., Papenbrock, T., Davda, M. M. and Awgulewitsch, A. (1994). The murine *HOXC* cluster contains five neighboring *AbdB*-related *Hox* genes that show unique spatially coordinated expression in posterior embryonic subregions. *Mech. Dev.* **47**, 253-260.

Popesko, P., Rajtova, V. and Horak, J. (1992). *A Color Atlas of the Anatomy of Small Laboratory Animals. 2: Rat, Mouse, Hamster*. London: Wolfe Publishing Ltd.

Rancourt, D. E., Tsuzuki, T. and Capecchi, M. R. (1995). Genetic interaction between *Hoxb-5* and *Hoxb-6* is revealed by nonallelic noncomplementation. *Genes Dev.* **9**, 108-122.

Rijli, F., Matyas, R., Pellegrini, M., Dierich, A., Gruss, P., Dollé, P. and Chambon, P. (1995). Cryptorchidism and homeotic transformations of spinal nerves and vertebrae in *Hoxa-10* mutant mice. *Proc. Natl. Acad. Sci. USA* **92**, 8185-8189.

Satokata, I., Benson, G. and Maas, R. (1995). Sexually dimorphic sterility phenotypes in *Hoxa10*-deficient mice. *Nature* **374**, 460-463.

Shubin, N. H. and Alberch, P. (1986). A morphogenetic approach to the the origin and basic organisation of the tetrapod limb. *Evol. Biol.* **20**, 319-387.

Small, K. M. and Potter, S. S. (1993). Homeotic transformations and limb defects in *Hoxa-11* mutant mice. *Genes Dev.* **7**, 2318-2328.

Sordino, P., van der Hoeven, F. and Duboule D. (1995) *Hox* gene expression in teleost fins and the origin of vertebrate digits. *Nature* **375**, 678-681.

(Accepted 22 November 1995)